General Disclaimer

One or more of the Following Statements may affect this Document

- This document has been reproduced from the best copy furnished by the organizational source. It is being released in the interest of making available as much information as possible.

- This document may contain data, which exceeds the sheet parameters. It was furnished in this condition by the organizational source and is the best copy available.

- This document may contain tone-on-tone or color graphs, charts and/or pictures, which have been reproduced in black and white.

- This document is paginated as submitted by the original source.

- Portions of this document are not fully legible due to the historical nature of some of the material. However, it is the best reproduction available from the original submission.

NASA CR-159444
TRW ER-8028

EXPLORATORY THERMAL-MECHANICAL FATIGUE RESULTS FOR RENE'80 IN ULTRAHIGH VACUUM

FINAL REPORT

OCTOBER 1978

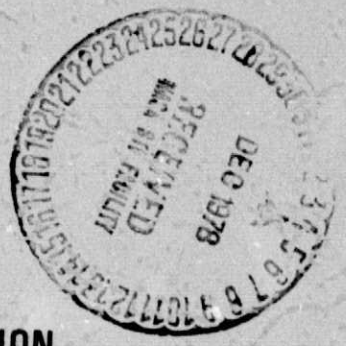

prepared for

NATIONAL AERONAUTICS AND SPACE ADMINISTRATION

UNDER CONTRACT NAS-3-21019

TRW MATERIALS TECHNOLOGY LABORATORIES
CLEVELAND, OHIO

1. Report No. NASA CR-159444	2. Government Accession No.	3. Recipient's Catalog No.
4. Title and Subtitle Exploratory Thermal-Mechanical Fatigue Results for Rene' 80 in Ultrahigh Vacuum		5. Report Date October 1978 6. Performing Organization Code
7. Author(s) A. A. Sheinker		8. Performing Organization Report No. TRW ER-8028
9. Performing Organization Name and Address TRW Inc. TRW Equipment 23555 Euclid Avenue Cleveland, Ohio 44117		10. Work Unit No. 11. Contract or Grant No. NAS-3-21019
12. Sponsoring Agency Name and Address NASA-Lewis Research Center 21000 Brookpark Road Cleveland, Ohio 44135		13. Type of Report and Period Covered FINAL 11 July 1977 - 11 July 1978 14. Sponsoring Agency Code

15. Supplementary Notes

Project Manager, G. R. Halford, Materials and Structures Division
NASA-Lewis Research Center
Cleveland, Ohio 44135

16. Abstract

A limited study was conducted of the use of strainrange partitioning for predicting the thermal-mechanical fatigue life of cast nickel-base superalloy Rene' 80. The fatigue lives obtained by combined in-phase thermal and mechanical strain cycling between 400°C (752°F) and 1000°C (1832°F) in an ultrahigh vacuum were considerably shorter than those represented by the four basic partitioned inelastic strainrange-fatigue life relationships established previously for this alloy at 871°C (1600°F) and 1000°C (1832°F) in an ultrahigh vacuum. This behavior was attributed to the drastic decrease in ductility with decreasing temperature for this alloy. These results indicated that the prediction of the thermal-mechanical fatigue life of Rene' 80 by the method of strainrange partitioning may be improved if based on the four basic fatigue life relationships determined at a lower temperature in the thermal-mechanical strain cycle.

17. Key Words (Suggested by Author(s))	18. Distribution Statement		
Nickel-Base Superalloys Rene' 80 Low Cycle Fatigue Creep Damage Strainrange Partitioning	Unclassified-Unlimited		
19. Security Classif. (of this report) Unclassified	20. Security Classif. (of this page) Unclassified	21. No. of Pages 21	22. Price*

* For sale by the National Technical Information Service, Springfield, Virginia 22161

FOREWORD

The work described in this report was performed in the Materials Technology Laboratory of TRW Inc. under the sponsorship of the National Aeronautics and Space Administration, Contract NAS-3-21019. The program was administered for TRW by Dr. C. S. Kortovich, Program Manager. The Principal Investigator was Dr. A. A. Sheinker, with technical assistance provided by Mr. J. W. Sweeney. The NASA Technical Manager was Dr. G. R. Haiford.

Prepared by: A. A. Sheinker
A. A. Sheinker
Engineer

Reviewed by: C S Kortovich
C. S. Kortovich
Section Manager
Physical Metallurgy

Approved by: J A Alexander
J. A. Alexander
Manager
Materials Research

TABLE OF CONTENTS

1 INTRODUCTION

Many critical engineering components, particularly those in gas turbine engines, are subjected to complex thermal and mechanical cycling during operation. The ability to predict the fatigue life under these conditions is necessary for the efficient, safe, and economical operation of these components. This is a difficult problem because it involves interactions between creep and fatigue, which are very complex (1,2). Considerable research has been conducted in this area in the past two decades and this has resulted in a number of methods of estimating the fatigue life of engineering materials under thermal-mechanical strain cycling (1,3-9).

One of the most promising approaches to the prediction of thermal-mechanical fatigue life of materials is the method of strainrange partitioning (9-13). In this technique, the inelastic strainrange in the cycle is divided into four basic components according to whether the strain is tensile or compressive, and time-independent (i.e, plastic) or time-dependent (i.e., creep). These four partitioned inelastic strainranges are defined as follows:

$\Delta\varepsilon_{pp}$ = tensile plastic strain reversed by compressive plastic strain.

$\Delta\varepsilon_{pc}$ = tensile plastic strain reversed by compressive creep strain.

$\Delta\varepsilon_{cp}$ = tensile creep strain reversed by compressive plastic strain.

$\Delta\varepsilon_{cc}$ = tensile creep strain reversed by compressive creep strain.

Relationships between each of these four basic types of inelastic strainrange and fatigue life are determined experimentally for the material, temperatures, and environment under consideration by conducting certain types of low-cycle fatigue tests designed to separate the four basic types of inelastic deformation. The thermal-mechanical strain cycle under consideration is partitioned into its four basic inelastic strainrange components (some of which may be zero), and the partitioned inelastic strainrange fractions are calculated from the relations,

$$F_{pp} = \Delta\varepsilon_{pp}/\Delta\varepsilon_{in}$$

$$F_{pc} = \Delta\varepsilon_{pc}/\Delta\varepsilon_{in}$$

$$F_{cp} = \Delta\varepsilon_{cp}/\Delta\varepsilon_{in}$$

$$F_{cc} = \Delta\varepsilon_{cc}/\Delta\varepsilon_{in}$$

where $\Delta\varepsilon_{in}$ is the total inelastic strainrange in the thermal-mechanical strain cycle. Cyclic lives N_{pp}, N_{pc}, N_{cp}, and N_{cc}, corresponding to the PP, PC, CP and CC types of inelastic deformation, respectively, are determined from the four experimentally obtained partitioned inelastic strainrange-fatigue life relationships at a strainrange equal to the total inelastic strainrange ($\Delta\varepsilon_{in}$) in the thermal-mechanical cycle. The predicted thermal-mechanical fatigue life is then calculated from the interaction damage rule,

$$\frac{1}{N_{pr}} = \frac{F_{pp}}{N_{pp}} + \frac{F_{pe}}{N_{pe}} + \frac{F_{ep}}{N_{ep}} + \frac{F_{ee}}{N_{ee}}$$

where N_{pr} is the predicted fatigue life.

The purpose of this program was to evaluate the applicability of the method of strainrange partitioning to thermal-mechanical fatigue of Rene' 80, a nickel-base superalloy. The four basic partitioned inelastic strainrange-fatigue life relationships for this alloy in both the uncoated and aluminide coated conditions at temperatures of 871°C (1600°F) and 1000°C (1832°F) in an ultrahigh vacuum had been determined in a previous program under NASA Contract NAS-3-17830 (14). Little difference was found between the life relationships for the uncoated and coated conditions and between the life relationships obtained at the two temperatures. However, the type of inelastic deformation strongly affected the life relationships. For a given partitioned inelastic strainrange, fatigue life decreased in the order PP, CC, CP and PC, with about an order of magnitude separating the longest (PP) and shortest (PC) cyclic lives. The objective of the present study was to determine whether the fatigue life of Rene' 80 subjected to a complex thermal-mechanical cycle can be predicted from these four basic fatigue life relationships using the method of strainrange partitioning.

II EXPERIMENTAL PROCEDURE

A. Material and Specimens

The material and specimens used in this study were the same as those used to determine the four basic partitioned inelastic strainrange-fatigue life relationships in the previous program (14). The Rene' 80 material was obtained from TRW master heat BL-5138, whose chemical composition is presented in Table 1. Tubular, hourglass-shaped specimens with threaded ends were individually cast as solid round bars and machined to the configuration shown in Figure 1, which is NASA Drawing CB-300740. Only uncoated specimens were employed in this program. Prior to finish grinding, the specimens were heat treated as follows:

1218°C (2225°F) for 2 hours in vacuum and argon quenched to room temperature.

1093°C (2000°F) for 4 hours in vacuum and argon quenched to room temperature

1052°C (1925°F) for 4 hours in vacuum, furnace cooled in vacuum to 649°C (1200°F) within 1 hour, and air cooled to room temperature (this simulates the coating cycle)

843°C (1550°F) for 16 hours in vacuum and furnace cooled to room temperature.

The resulting microstructure had an ASTM grain size of 3.

B. Fatigue Tests

This program involved a total of 12 fatigue tests. Seven of these were thermal-mechanical fatigue tests with thermal cycling in-phase (TCIP). These consisted of programmed thermal-mechanical strain cycling with temperature increasing as tensile axial strain increased and temperature decreasing as compressive axial strain increased. The other five were pure thermal cycling with no applied mechanical strain or load.

The equipment and procedures used for the vacuum fatigue tests in this program have been described in detail previously (15,16). Briefly, the test apparatus was designed to perform completely reversed push-pull fatigue tests on hourglass-shaped specimens using independently programmable temperature and strain control. Temperature was programmed using a thyratron-controlled 50-KV-AC transformer for direct resistance heating of the specimen, while diametral strain was controlled directly using an LVDT-type extensometer coupled to a programmable, closed-loop, electrohydraulic servosystem. The temperature of the specimen was measured using thermocouples spot-welded directly to the specimen surface. Load, diameter, and temperature were recorded continuously and load-diameter hysteresis loops were obtained at periodic intervals during each test.

Table I

Chemical Composition of Rene' 80 Material Used for Thermal-Mechanical Fatigue Tests, Weight Percent

Element	TRW Master Heat BL 5138	Nominal Composition*
C	0.17	0.17
Si	<0.05	-
Mn	<0.02	-
Cr	13.80	14.0
Mo	4.11	4.0
Fe	0.13	-
Ti	4.87	5.0
Al	2.99	3.0
Co	9.73	9.5
W	3.94	4.0
Zr	0.043	0.03
B	0.015	0.015
Ni	Balance	Balance

* Per ASTM Data Series Publication No. DS9E.

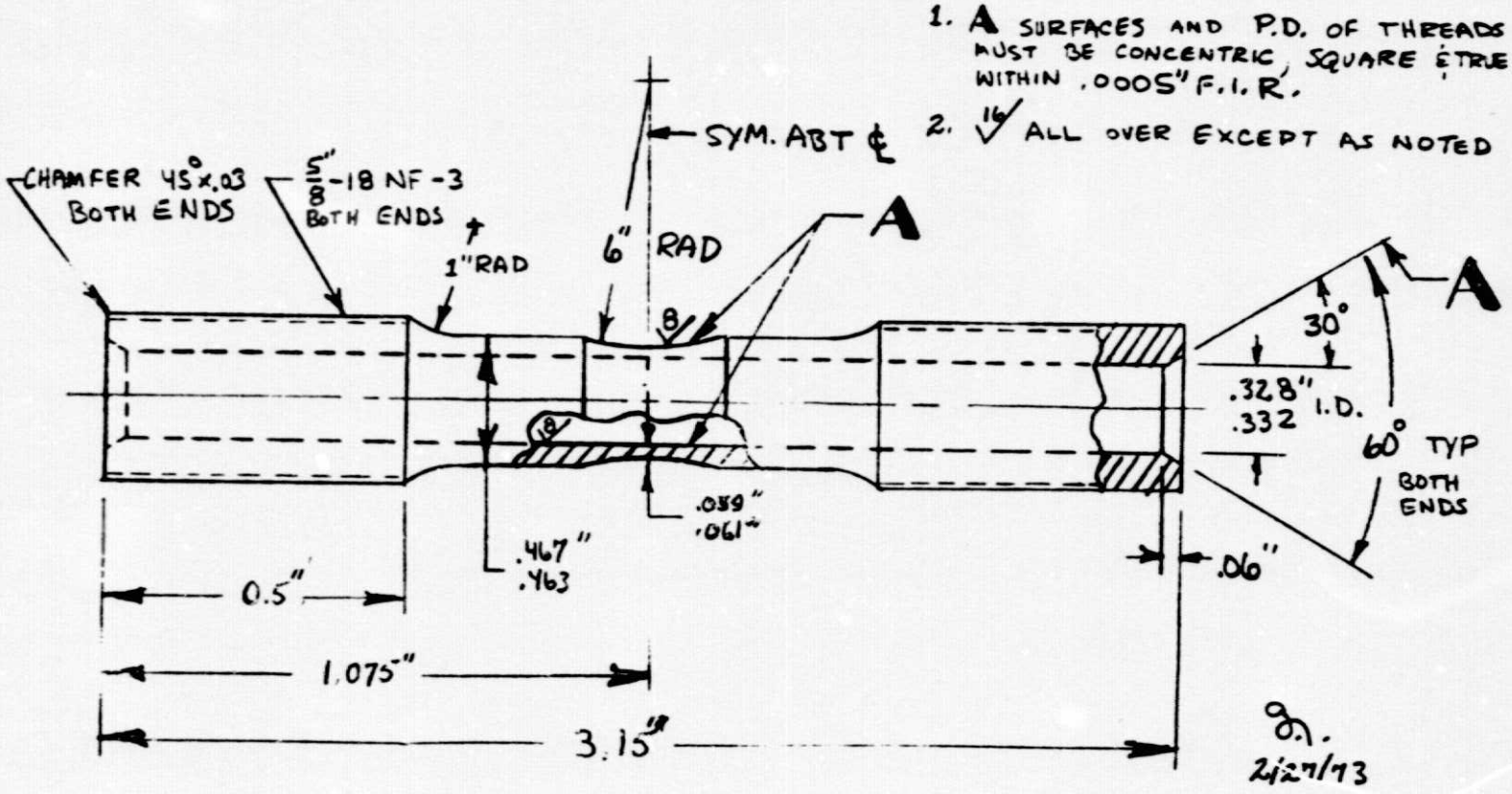

Figure 1. Fatigue test specimen

In the thermal-mechanical fatigue tests, the mechanical strain was cycled linearly with time, resulting in a triangular strain-time wave shape. The temperature of the specimen was programmed such that the diametral thermal expansion cycled linearly with time, resulting in a slightly nonlinear variation of temperature with time, as shown in Figure 2. This was necessary to keep mechanical strain and temperature in phase, because the thermal expansion of this alloy was not linear with temperature, the diametral thermal expansion was much greater than the diametral mechanical strain in these tests, and the diametral extensometer controlled the algebraic sum of diametral thermal expansion and diametral mechanical strain. The temperature was cycled between 400°C (752°F) and 1000°C (1832°F). In the pure thermal cycling tests, the temperature was cycled in the same manner, either between 400°C (752°F) and 1000°C (1832°F) or between 243°C (470°F) and 843°C (1550°F). Both the thermal-mechanical and the pure thermal cycling tests were conducted with a 12-minute cycle, resulting in a cyclic frequency of 0.0014 hz. All of the fatigue tests were performed in an ultrahigh vacuum of 10^{-4} torr or less to eliminate environmental effects. Fatigue failure was defined in all cases as complete separation of the specimen into two pieces.

The step-stress method (13,17) of experimentally separating the total inelastic strainrange into plastic and creep components was utilized in the thermal-mechanical fatigue tests. In this technique, the component of steady-state creep for the entire period of the time interval considered is taken as the "creep" strain for use in the strainrange partitioning analysis. All of the remaining inelastic strain, whether instantaneous or occurring as first stage (primary) creep, is taken to be "plastic" strain. The temperature and strain programmers are temporarily halted at a selected point on the stabilized load (stress) - diameter (strain) hysteresis loop, the servocontroller is switched from strain to load control, and the stress and temperature are held constant at the stabilized values associated with the selected point while the creep strain is measured as a function of time. This condition is maintained until a reasonably linear creep rate is established. This is taken as an approximation to the steady-state creep condition. The servocontroller is then switched back to strain control and the strain and temperature programs are resumed. This procedure is repeated at a series of selected points around the stabilized hysteresis loop. Before stopping at each step-stress level, the hysteresis loop is restabilized by traversing one or more cycles until the loop repeats the path of the previous loops. A plot of the steady-state creep rate versus time within the thermal-mechanical cycle corresponding to each selected step-stress point is then constructed. The amounts of tensile and compressive creep strain are determined by integrating the areas under the resulting curves, with areas above the horizontal (time) axis representing tensile creep and areas below the horizontal axis representing compressive creep.

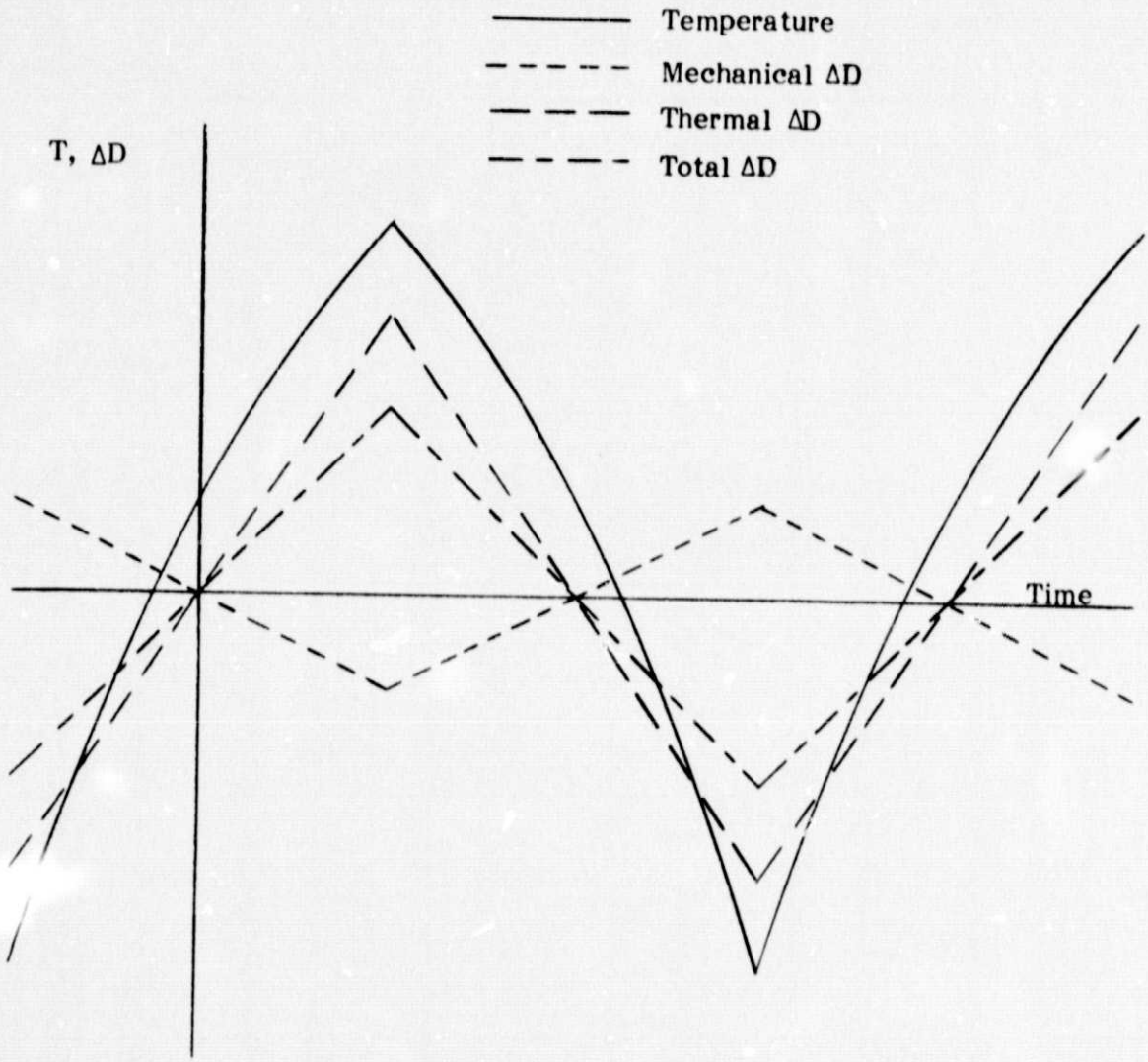

Figure 2. Schematic illustration of temperature-time and diametral displacement (Δ D)- time wave shapes (in-phase shown).

III. RESULTS AND DISCUSSION

The fatigue test results are presented in Table 2. The axial inelastic strainrange was determined as follows. The width of a representative (approximately half-life) load-diameter hysteresis loop was measured at the zero-load level and converted to gross diametral displacement by multiplying by the horizontal scale factor for the X-Y recorder and the calibration factor for the diametral extensometer. This product was divided by the outside diameter of the specimen to obtain gross diametral strain. Since both the diametral thermal expansion and the diametral mechanical strain varied linearly with time within the thermal-mechanical cycle, thermal expansion was eliminated from the gross diametral strain by multiplying the latter by the ratio of the mechanical strain control setting to the gross strain control setting. This product was the diametral inelastic strainrange, which was then multiplied by -2 to obtain the axial inelastic strainrange. For example, for test number 7:

(1) width of representative load-diameter hysteresis loop at zero load =

$W = 0.079$ m. (3.1 in.)

(2) horizontal scale factor for X-Y recorder =

$F_X = 394$ mv./m. (10.0 mv./in.)

(3) calibration factor for diametral extensometer =

$F_E = 1.47 \times 10^{-6}$ m./mv. (58×10^{-6} in/mv.)

(4) gross diametral displacement =

$$\begin{aligned} D &= (W)(F_X)(F_E) \\ &= (0.079 \text{ m.})(394 \text{ mv./in.})(1.47 \times 10^{-6} \text{ m./mv.}) \\ &= (3.1 \text{ in.})(10 \text{ mv./in.})(58 \times 10^{-6} \text{ in./mv.}) \\ &= 0.0000458 \text{ m. } (0.00180 \text{ in.}) \end{aligned}$$

(5) outside diameter of specimen =

$D_o = 0.0114$ m. (0.449 in.)

(6) gross diametral strain =

$$\Delta\varepsilon \text{ gross} = \frac{\Delta D}{D_o} = \frac{0.0000458 \text{ m.}}{0.0114 \text{ m.}} = \frac{0.00180 \text{ in.}}{0.449 \text{ in.}} = 0.004002$$

(7) mechanical strain control setting = -2.5 mv.

(8) thermal expansion control setting = 96.0 mv.

Table 2

Thermal-Mechanical Fatigue Test Results for Rene' 80 in Ultrahigh Vacuum

Test Number	Specimen Number	Test Type	Axial Strainrange			Peak Tensile Stress		Peak Compressive Stress		Cycles to Failure	Remarks
			Total	Elastic	Inelastic	MPa	ksi	MPa	ksi		
1	REE-231	TCIP	-	-	-	-	-	-	-	1	Strainrange too high
2	REE-232	TCIP	-	-	-	-	-	-	-	4	Strainrange too high
3	REE-233	TCIP	0.00510	0.00457	0.00053	193	28.0	611	88.6	95	Power interrupted
4	REE-234	TCIP	0.00535	0.00482	0.00053	154	22.4	708	102.7	43	Equipment malfunctioned
5	REE-235	TCIP	0.00596	0.00511	0.00085	224	32.5	672	97.5	45	Insufficient creep data
6	REE-236	TCIP	0.00493	0.00447	0.00046	129	18.7	676	98.0	61	Insufficient creep data
7	REE-238	TCIP	0.00437	0.00416	0.00021	161	23.3	576	83.5	158	
8	REE-239	Pure Thermal	0	0		0	0	0	0	-	400 to 1000°C cycle; power interrupted after 12 cycles
9	REE-240	Pure Thermal	0	0	0	0	0	0	0	-	400 to 1000°C cycle; suspended after 1260 cycles
10	REE-228	Pure Thermal	0	0	0	0	0	0	0	-	243 to 843°C cycle; equipment malfunctioned after 245 cycles
11	REE-230	Pure Thermal	0	0	0	0	0	0	0	-	243 to 843°C cycle; equipment malfunctioned on first cycle
12	REE-242	Pure Thermal	0	0	0	0	0	0	0	-	243 to 843°C cycle; suspended after 1007 cycles

(9) gross strain control setting =

$$-2.5 \text{ mv.} + 96.0 \text{ mv.} = 93.5 \text{ mv.}$$

(10) diametral inelastic strainrange =

$$\Delta\epsilon \text{ diam. inel.} = \frac{-2.5 \text{ mv.}}{93.5 \text{ mv.}} \; (\Delta\epsilon \text{ gross})$$

$$= \frac{-2.5 \text{ mv.}}{93.5 \text{ mv.}} \; (0.004002)$$

$$= -0.000107$$

(11) axial inelastic strainrange =

$$\Delta\epsilon \text{ axial inel.} = (-2)(\Delta\epsilon \text{ diam. inel.})$$

$$= (-2)(-0.000107)$$

$$= 0.00021$$

The axial elastic strainrange was calculated by adding the peak tensile elastic strain and the peak compressive elastic strain. The former was obtained by dividing the peak tensile stress by the modulus of elasticity at the maximum temperature in the cycle, 1000°C (1832°F), while the latter was obtained by dividing the peak compressive stress by the modulus of elasticity at the minimum temperature in the cycle, 400°C (752°F). For example, for test number 7:

(1) peak tensile stress =

$$\sigma_t = 161 \text{ MPa } (23.3 \text{ ksi})$$

(2) modulus of elasticity at 1000°C =

$$E_{1000} = 144{,}000 \text{ MPa } (20{,}900 \text{ ksi})$$

(3) peak tensile elastic strain =

$$\epsilon_t = \frac{\sigma_t}{E_{1000}} = \frac{161 \text{ MPa}}{144{,}000 \text{ MPa}} = \frac{23.3 \text{ ksi}}{20{,}900 \text{ ksi}} = 0.00111$$

(4) peak compressive stress =

$$\sigma_c = 576 \text{ MPa } (83.5 \text{ ksi})$$

(5) modulus of elasticity at 400°C =

$$E_{400} = 189{,}000 \text{ MPa } (27{,}400 \text{ ksi})$$

(6) peak compressive elastic strain =

$$\epsilon_c = \frac{\sigma_c}{E_{400}} = \frac{576 \text{ MPa}}{189{,}000 \text{ MPa}} = \frac{83.5 \text{ ksi}}{27{,}400 \text{ ksi}} = 0.00305$$

(7) axial elastic strainrange =

$$\Delta\epsilon_{el} = \epsilon_t + \epsilon_c$$

$$= 0.00111 + 0.00305$$

$$= 0.00416$$

The axial total strainrange was simply the sum of the axial elastic strainrange and the axial inelastic strainrange.

The fatigue lives for the three completed thermal-mechanical fatigue tests (numbers 5, 6, and 7) are plotted as a function of axial inelastic strainrange in Figure 3, along with the four basic partitioned inelastic strainrange-fatigue life relationships established previously for this alloy at 871°C (1600°F) and 1000°C (1832°F) (14). According to the method of strainrange partitioning, the highest (PP) and lowest (PC) lines representing these basic fatigue life relationships provide upper and lower bounds, respectively, on fatigue life. This means that, for a given inelastic strainrange, the longest possible fatigue life would result from a strain cycle in which the inelastic strain consists entirely of the PP type, while the shortest possible fatigue life would result from a strain cycle in which the inelastic strain consists entirely of the PC type. A complex strain cycle in which the inelastic strain consists of a combination of two or three of the four basic types of inelastic deformation (both PC and CP types cannot occur in a given cycle) would result in a fatigue life somewhere between those represented by the PP and PC lines. Thus, if the thermal-mechanical fatigue life of Rene' 80 can be predicted from these four basic fatigue life relationships using the method of strainrange partitioning, the thermal-mechanical fatigue data should be bounded by the PP and PC lines. However, the fatigue lives for the three completed thermal-mechanical fatigue tests were considerably shorter than those represented by the lower bounding PC line at the same levels of inelastic strainrange. This suggests that the four basic fatigue life relationships for Rene' 80 at 871°C (1600°F) and 1000°C (1832°F) may not be appropriate for using the method of strainrange partitioning to predict the thermal-mechanical fatigue life of this alloy cycled between 400°C (752°F) and 1000°C (1832°F). The reason for this anomaly was investigated.

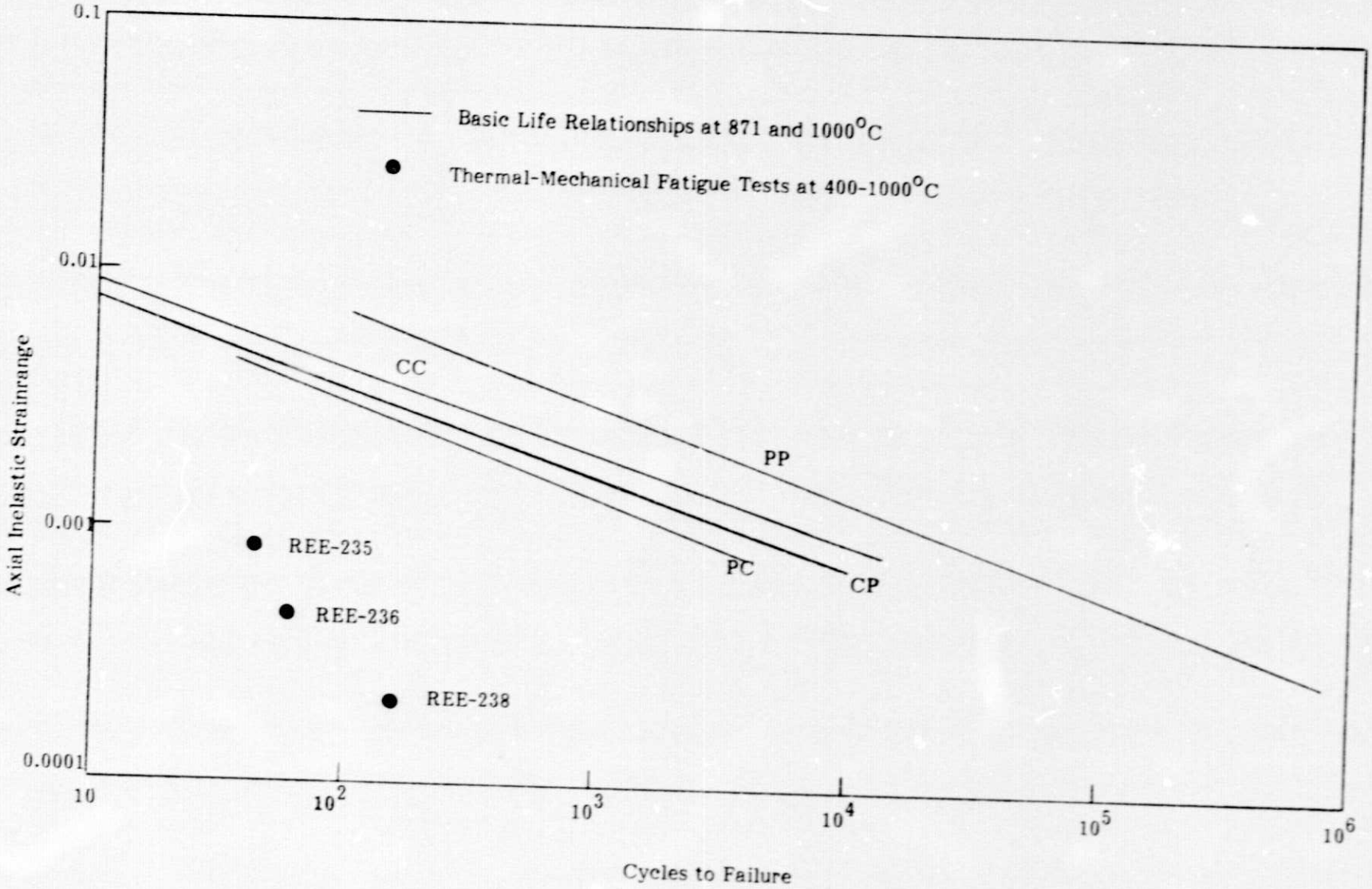

Figure 3. Comparison of thermal-mechanical fatigue test results with the four basic partitioned inelastic strainrange-fatigue life relationships for Rene' 80.

In order to determine whether the thermal cycling alone was very damaging to this alloy, pure thermal cycling tests were conducted. In one of these tests (number 9), the specimen was thermally cycled over the same temperature range as that employed in the thermal-mechanical fatigue tests, 400°C (752°F) to 1000°C (1832°F), and no failure occurred in 1260 cycles. Another pure thermal cycling test (number 12) was conducted over the temperature range from 243°C (470°F) to 843°C (1550°F) to determine whether thermal cycling at lower temperatures, but with the same temperature variation as that used in the thermal-mechanical fatigue tests, 600°C (1110°F), would be damaging to this alloy. In this test, no failure occurred in 1007 cycles. Both of these specimens were then tensile tested at room temperature to determine whether the thermal cycling had affected the mechanical properties. These results are presented in Table 3. In both specimens, the ultimate tensile strength and the ductility, as indicated by the reduction of area, were much lower than the values reported previously for Rene' 80 at room temperature (18). To establish whether the original tensile properties of this material were typical of Rene' 80, tensile tests were conducted at room temperature and 899°C (1650°F) on specimens which had not been thermally cycled. As shown in Table 3, the ultimate tensile strength at room temperature and the reduction of area at both temperatures were much lower than the corresponding values reported previously for this alloy (18). However, the room temperature tensile properties were about the same as those obtained after thermal cycling. Thus, the tensile properties of this material were not impaired by the thermal cycling, but were lower than normal for Rene' 80. This suggests why the thermal-mechanical fatigue lives were considerably shorter than would be predicted from the four basic fatigue life relationships.

The low-cycle fatigue resistance of an alloy generally decreases with decreasing ductility (19). Since the ductility of the Rene' 80 material decreased with decreasing temperature, the low-cycle fatigue life of this material at a given inelastic strainrange would be expected to decrease with decreasing temperature. This would shift the four basic fatigue life relationships for this material to lower levels of inelastic strainrange and/or fatigue life at lower temperatures (20). Since the thermal-mechanical fatigue tests in the present study were conducted over the temperature range from 400°C (752°F) to 1000°C (1832°F), the thermal-mechanical fatigue life was probably greatly affected by the lower temperatures in this range. The ductility of certain nickel-base superalloys such as Rene' 80 can also be reduced by prolonged exposure to elevated temperature because of time-dependent microstructural changes (21), and this degradation could be accelerated by thermal cycling. The decrease in ductility with decreasing temperature suggests that the prediction of the thermal-mechanical fatigue life of Rene' 80 by the method of strainrange partitioning may be improved if based on the four basic fatigue life relationships determined at a lower temperature in the thermal-mechanical strain cycle.

Table 3

Tensile Properties of Rene' 80

Specimen Number	Test Temperature °C	Test Temperature °F	Yield Strength at 0.2% Offset MPa	Yield Strength at 0.2% Offset ksi	Ultimate Tensile Strength MPa	Ultimate Tensile Strength ksi	Reduction of Area %	Notes
Tensile Test Results								
REE-240	25	77	-	-	820	119	3.4	After 1260 thermal cycles, 400-1000°C
REE-242	25	77	-	-	786	114	3.1	After 1007 thermal cycles, 243-843°C
REE-237	25	77	689	100	731	106	1.2	
REE-241	25	77	820	119	869	126	3.1	
REE-247	899	1650	-	-	-	-	11.7	Air test at NASA-Lewis
REE-249	899	1650	336	48.8	717	104	2.6	" " " " "
REE-209	1000	1832	266	38.6	425	61.6	35.4	" " " " "
REE-244	1000	1832	-	-	415	60.2	31.3	" " " " "
Previously Reported Properties								
-	21	70	821	119	996	144	6.2	Ref. 18
-	850	1562	538	78.0	683	99.0	29.4	Ref. 18
-	925	1697	359	52.0	509	73.9	33.2	Ref. 18
-	1000	1832	230	33.3	333	48.3	32.7	Ref. 18

IV SUMMARY

A limited study was conducted of the use of strainrange partitioning as a method of predicting the fatigue life of cast nickel-base superalloy Rene' 80 under combined thermal and mechanical strain cycling. The four basic partitioned inelastic strainrange-fatigue life relationships for this alloy had been established previously at 871°C (1600°F) and 1000°C (1832°F) in an ultrahigh vacuum. Thermal-mechanical fatigue tests were conducted on Rene' 80 specimens in an ultrahigh vacuum using thermal cycling in-phase (TCIP) between 400°C (752°F) and 1000°C (1832°F). The thermal-mechanical fatigue lives were considerably shorter than those represented by the lower bound of the four basic fatigue life relationships, suggesting that these particular four relationships may not be appropriate for using the method of strainrange partitioning to predict the fatigue life of this alloy under thermal-mechanical cycling over this temperature range. This anomaly was attributed to a decrease in ductility with decreasing temperature for this alloy, since low-cycle fatigue resistance generally decreases with decreasing ductility. The results indicated that the prediction of the thermal-mechanical fatigue life of Rene' 80 by the method of strainrange partitioning may be improved if based on the four basic fatigue life relationships determined at a lower temperature in the thermal-mechanical strain cycle.

V REFERENCES

1. S. S. Manson, "Interfaces Between Fatigue, Creep, and Fracture," Intl. Journal of Fracture Mechanics, Vol. 2, March 1966, pp. 327-363.

2. E. G. Ellison, "A Review of the Interaction of Creep and Fatigue," Journal of Mech. Eng. Science, Vol. 11, June 1969, pp. 318-339.

3. S. Taira, "Lifetime of Structures Subjected to Varying Load and Temperature," Creep in Structures, N. J. Hoff, ed., Springer-Verlag, Berlin, 1962, pp. 96-119.

4. S. S. Manson and D. A. Spera, Discussion of "Low-Cycle Fatigue Damage of Udimet 700 at 1400°F," by C. H. Wells and C. P. Sullivan, ASM Trans. Quart., Vol. 58, 1965, pp. 749-751.

5. S. S. Manson and G. R. Halford, " A Method of Estimating High-Temperature Low-Cycle Fatigue Behaviour of Materials," Thermal and High Strain Fatigue, The Metals and Metallurgy Trust, London, 1967, pp. 154-170.

6. D. A. Spera, "A Linear Creep Damage Theory for Thermal Fatigue of Materials," Ph.D. Thesis, University of Wisconsin, 1968.

7. L. F. Coffin, "Predictive Parameters and Their Application to High-Temperature Low-Cycle Fatigue," Fracture 1969, Chapman and Hall, London, 1969, pp.643-654.

8. J. R. Ellis and E. P. Esztergar, "Considerations of Creep-Fatigue Interaction in Design Analysis," Symposium on Design for Elevated Temperature Environment, American Society of Mechanical Engineers, New York, 1971, pp. 29-43.

9. S. S. Manson, G. R. Halford, and M. H. Hirschberg, "Creep-Fatigue Analysis by Strain-Range Partitioning," Symposium on Design for Elevated Temperature Environment, American Society of Mechanical Engineers, New York, 1971, pp. 12-24.

10. G. R. Halford, M. H. Hirschberg, and S. S. Manson, "Temperature Effects on the Strainrange Partitioning Approach for Creep Fatigue Analysis," Fatigue at Elevated Temperatures, ASTM STP 520, American Society for Testing and Materials, Philadelphia, 1973, pp. 658-669.

11. S. S. Manson, "The Challenge to Unify Treatment of High Temperature Fatigue-A Partisan Proposal Based on Strainrange Partitioning," Fatigue at Elevated Temperatures, ASTM STP 520, American Society for Testing and Materials, Philadelphia, 1973, pp. 744-782.

12. M. H. Hirschberg and G. R. Halford, "Use of Strainrange Partitioning to Predict High-Temperature Low-Cycle Fatigue Life," NASA Technical Note No. D-8072, January 1976.

13. G. R. Halford and S. S. Manson, "Life Prediction of Thermal-Mechanical Fatigue Using Strainrange Partitioning," Thermal Fatigue of Materials and Components, ASTM STP 612, D. A. Spera and D. F. Mowbray, eds., American Society for Testing and Materials, Philadelphia, 1976, pp. 239-254.

14. C. S. Kortovich, "Ultrahigh Vacuum, High Temperature, Low Cycle Fatigue of Coated and Uncoated Rene' 80," NASA Report No. NAS-CR-135003, TRW Report No. ER-7861, April 1976.

15. K. D. Sheffler and G. S. Doble, "Influence of Creep Damage on the Low Cycle Thermal-Mechanical Fatigue Behavior of Two Tantalum Base Alloys," NASA Report No. NAS-CR-121001, TRW Report No. ER-7592, May 1, 1972.

16. K. D. Sheffler and G. S. Doble, "Thermal Fatigue Behavior of T-111 and ASTAR 811C in Ultrahigh Vacuum," Fatigue at Elevated Temperatures, ASTM STP 520, American Society for Testing and Materials, Philadelphia, 1973, pp. 491-499.

17. S. S. Manson, G. R. Halford, and A. J. Nachtigall, "Separation of the Strain Components for Use in Strainrange Partitioning," Advances in Design for Elevated Temperature Environment, American Society of Mechanical Engineers, New York, 1975, pp. 17-28.

18. L. J. Fritz and W. P. Koster, "Tensile and Creep Rupture Properties of (16) Uncoated and (2) Coated Engineering Alloys at Elevated Temperatures," NASA Report No. NAS-CR-135138, Metcut Research Associates Report No. 931-21300, January 15, 1977.

19. S. S. Manson, "Fatigue: A Complex Subject - Some Simple Approximations," Experimental Mechanics, Vol. 5, No. 7, July 1965, pp. 193-226.

20. G. R. Halford, J. F. Saltsman, and M. H. Hirschberg, "Ductility Normalized-Strainrange Partitioning Life Relations for Creep-Fatigue Life Predictions," Proceedings of Conference, Environmental Degradation of Engineering Materials, M. R. Louthan, Jr., and R. P. McNitt, eds., College of Engineering, Virginia Tech, Blacksburg, Virginia, 1977, pp. 599-612.

21. W. H. Chang, "Tensile Embrittlement of Turbine Blade Alloys After High-Temperature Exposure," Superalloys--Processing, Proceedings of the Second International Conference, Metals and Ceramics Information Center, Battelle Columbus Laboratories, Columbus, Ohio, 1972.

DISTRIBUTION LIST

Techn Info Ctr
AEG
General Electric Co
Cincinnati, OH 45215

Library
Detroit Diesel Allison
340 White Rover Pkwy
Indianapolis, IN 46206

Library
Denver Research Institute
University Park
Denver, CO 80210

Library
Southern Research Inst.
2000 Ninth Ave South
Birmingham, AL 35205

Braden, R C
Mech Prop Data Ctr
Belfour Stulen Div
13919 W Bay Shore Dr
Traverse City, MI 49684

Schaefer, A O
M P C
United Engineering Center
345 E 47th St
New York, NY 10017

Technical Library
Sargent & Lundy
Room 27P48
55 E Monroe St
Chicago, IL 60603

Aerojet Liquid Rocket Ctr
Tech Info Ctr 7362
c/o R Duncan
Box 1322
Sacramento, CA 95813

Technical Library
Hamilton Standard
Div of United Tech Corp
Windsor Locks, CT 06096

Technical Library
SKF Industries
1100 First Ave
King of Prussia, PA 19406

R&D Library
Huntington Alloy Prod Div
International Nickel
Huntington, WV 25720

Technical Library
Lockheed-California
Burbank, CA 91503

Technical Library
McDonnell-Douglas Corp
Missiles & Space Div
5301 Bolsa Ave
Huntington Beach CA 92647

Technical Library
Rockwell Int'l
6633 Canoga Ave
Canoga Pk, CA 91304

Technical Library
Northrop Corp
Aircraft Div
3901 West Broadway
Hawthorne, CA 90250

Technical Library
Philco-Ford Corp
Ford Road
Newport Beach, CA 92663

Technical Library
Sandia Corp
Albuquerque, NM 87115

Technical Library
AVCO-Space Systems Div
Lowell Industrial Pk
Lowell, MA 01851

Technical Library
Beech Aircraft
Wichita, KS 67201

Technical Library
Douglas Aircraft Co
3852 Lakewood Blvd
Long Beach, CA 90801

Technical Library
G E
1000 Western Ave
Lynn, MA 01905

Technical Library
AR&TL
Fort Eustis, VA 23604

Technical Library
Solar
Div of Int'l Harvester
2200 Pacific Hwy
San Diego, CA 92101

Technical Library
General Atomic
Box 1259
Morristown, NJ 07960

Technical Library
Foster Wheeler Corp
12 Peach Tree Hill Rd
Livingston, NJ 07039

Technical Library
Boeing
3801 S Oliver
Wichita, KS 67210

Library - Tech Ctr
Fisher Controls Co
205 S Center St
Marshalltown, IA 50158

Technical Library
Southwest Research
8500 Culebra Rd
San Antonio, TX 78284

Defense Documentation Ctr
Cameron Station
5010 Duke St
Alexandria, VA 22314

MCIC
Battelle Memorial Inst
505 King Ave
Columbus, OH 43201

Tech Reports Library (3)
D O E
Washington, DC

Tech Info Service (3)
D O E
Box 62
Oak Ridge, TN

Library MS-185
NASA
Langley Research Ctr
Langley Field, VA 23365

Library
NASA
Marshall Space Flight Ctr
Huntsville, AL 35812

Tech Library / JM6
NASA
Manned Spacecraft Ctr
Houston, TX 77058

Library - Acquisitions
NASA - JPL
4800 Oak Grove Dr
Pasadena, CA 91102

Library
NASA
Goddard Space Flight Ctr
Greenbelt, MD 20771

Library
NASA
Flight Research Ctr
P O Box 273
Edwards, CA 93523

Library MS 202-3
NASA
Ames Research Ctr
Moffett Field, CA 94035

Technical Library
AFML/LAM
WPAFB, OH 45433

Research Library
United Tech Corp
400 Main St
E Hartford, CT 06108

Library
P&WA
United Tech Corp
W Palm Beach, FL 33402

Library
G E Co
Box 8
Schenectady, NY 12301

Technology Utilization
NASA MS 3-19
Lewis Research Ctr
Cleveland, OH 44135

Report Control Office
NASA MS 5-5
Lewis Research Ctr
Cleveland, OH 44135

Patent Council
NASA MS 500-311
Lewis Research Ctr
Cleveland, OH 44135

Library (2)
NASA MS 60-3
Lewis Research Ctr
Cleveland, OH 44135

AGTS Contracts Sect
NASA MS 500-312
Lewis Research Ctr
Cleveland, OH 44135

AR&TL Office
MS 77-5
NASA Lewis Research Ctr
Cleveland, OH 44135

APSC Liaison Office
MS 501-3
NASA Lewis Research Ctr
Cleveland, OH 44135

Halford, Dr Gary R (85)
MS 49-1, NASA-Lewis
21000 Brookpark Rd
Cleveland, OH 44135